

Hybrid Computation of Flow-Induced Noise using the FE Method

Max Escobar¹, Simon Triebenbacher¹, Manfred Kaltenbacher¹,
Irfan Ali², Stefan Becker², Reinhard Lerch¹

¹ Dept. of Sensor Technology (LSE), Paul-Gordan-Str. 3/5, 91052 Erlangen. Email: max.escobar@lse.eei.uni-erlangen.de

² Institute of Fluid Mechanics (LSTM), Cauerstr. 12, 91058 Erlangen

Introduction

We present a numerical scheme for the efficient simulation of flow-induced noise. In the hybrid approach, turbulent flow fields computed with Large Eddy Simulation (LES) or Scale Adaptive Simulation (SAS) turbulence methods are used to evaluate the acoustic sources. For the computation of the radiated sound field we solve Lighthill's acoustic analogy by means of the Finite Element Method (FEM). Figure 1 depicts the general hybrid approach used for the computation where Ω_1 and Ω_2 encompass the acoustic propagation region. In the coupled region Ω_1 , corresponding to the fluid domain, different discretizations are used on both sides of the computation and interpolation of the data is performed employing a conservative scheme. Acoustic sources are computed by means of the FE method from the velocity components directly on the fine fluid mesh. The resulting scalar values are interpolated as acoustic nodal loads to the acoustic grid. The acoustic propagation can be solved both in time and in frequency domain. In the latter analysis, the Perfectly Matched Layer (PML) method is employed, which efficiently reduces reflections on the acoustic boundary. Finally, the implementation is validated and numerical examples are presented of the sound generated by turbulent flows around cylinders with different geometric configurations. Besides the numerical investigations, measurements for the same configurations are carried out in an aeroacoustic wind tunnel located at our department.

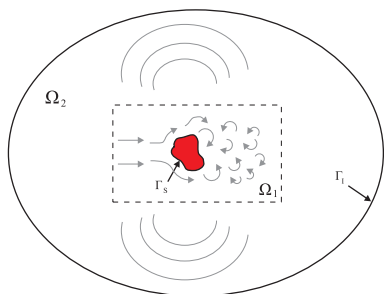


Figure 1: Set-up for the flow-induced noise computation

Theoretical Approach

We perform a volume discretization of Lighthill's equation [2] by applying the Finite Element Method. Therewith, the interactions of any solid/elastic body with the turbulent flow field will be implicitly taken into account by the variational formulation of the PDE. The governing equation for our aeroacoustic problem is given by the

original Lighthill's inhomogeneous wave equation which reads

$$\frac{\partial^2 \rho'}{\partial t^2} - c_0^2 \frac{\partial^2 \rho'}{\partial x_i^2} = \frac{\partial^2 T_{ij}}{\partial x_i \partial x_j}, \quad (1)$$

with ρ' representing the acoustic density fluctuation and T_{ij} the components of the Lighthill tensor $[T]$ approximated as $T_{ij} \approx \rho u_i v_j$.

Numerical Investigation

Initially, the implementation is validated employing the analytical solution for the acoustic field induced by a co-rotating vortex pair and comparing it with the numerical results computed following the hybrid approach. Figure 2 compares the decay of the acoustic pressure along the positive x-axis between the numerical and analytical values. A good agreement is found between the numerical and analytical values, with only slightly lower amplitudes in the former case which are mainly due to the discrete evaluation of the acoustic sources.

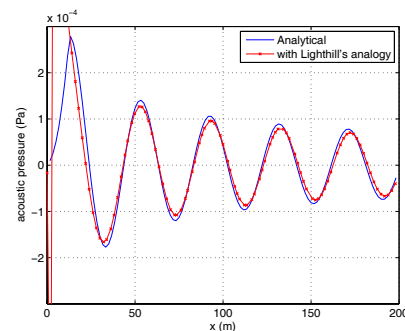


Figure 2: Decay of the acoustic pressure values along the x-axis

Additionally, a 2D computation of the flow-induced noise generated by a square cylinder has been computed, in both transient and frequency domains, in order to evaluate the performance of the PML and the sensitivity of the conservative interpolation of the quantities. Acoustic sources in this case have been obtained from a simplified 3D LES fluid computation with $Re = 13000$. Directivity plots from the transient and harmonic analyses at a radius $r = 1$ m away from the cylinder are compared in Fig. 3. Only small numerical differences are present, mainly due to the evaluation of the amplitudes from the transient pressure signals and due to slight differences in the grids

used in the transient and harmonic computations. The use of PML in the harmonic computation provides very good absorption, allowing the use of a small numerical domain, which in all directions encompasses just a fraction of the acoustic wave length for the main frequency component (about $\lambda/3$ where for $f = 65$ Hz, $\lambda = 5.27$ m).

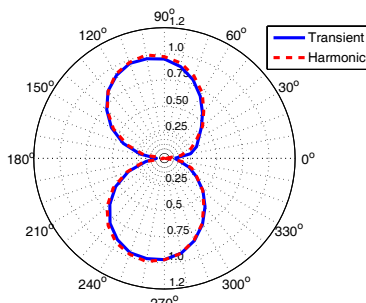


Figure 3: Comparison of directivity patterns at $r = 1.0$ m

In the 3D case, numerical results are presented for the flow-induced noise from wall-mounted cylinders with different geometry profiles as shown in Fig. 4, both cases resulting in a Reynolds number around 13000 based on the crossflow side length of $L = 20$ mm. For the evaluation of the acoustic sources CFD results from SAS computations carried out with ANSYS-CFX have been used. These configurations have also been investigated experimentally in the anechoic chamber at our department.

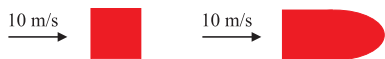


Figure 4: Profiles of wall-mounted cylinder geometries

Isosurfaces plots for the square cylinder and the cylinder with elliptic profile are presented in Figures 5 and 6, respectively (dots depict PML). Significantly higher amplitudes are present in the results for the elliptic profile.

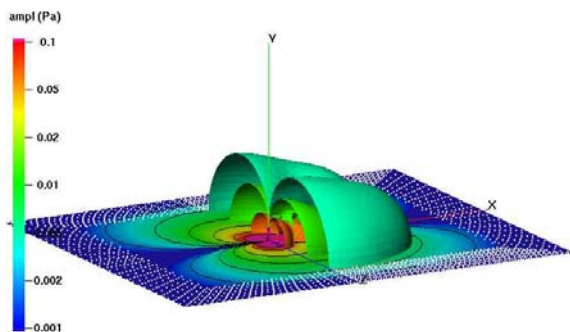


Figure 5: Isosurface of acoustic pressure for wall-mounted square cylinder at $f = 55$ Hz, clipped at yz -plane

Directivity plots of the SPL levels at a radius $r = 1$ m away from the wall mounted cylinders are presented in Fig. 7. A good qualitative and quantitative agreement

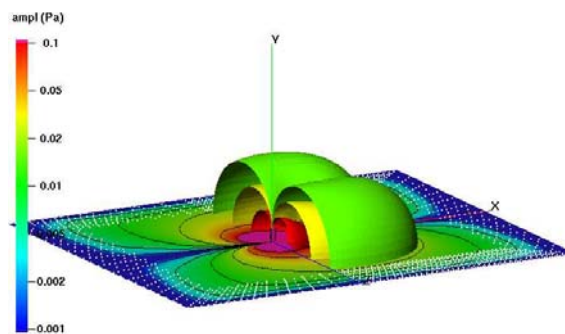


Figure 6: Isosurface of acoustic pressure for wall-mounted square cylinder with elliptic profile at $f = 39$ Hz, clipped at yz -plane

in frequencies and amplitudes is found with experiments for the same inflow velocity $v = 10$ m/s presented in [1]. The SPL difference between both cases at 0° on the yz -plane accounts for 16dB in the experiments and 14dB in the numerical computations.

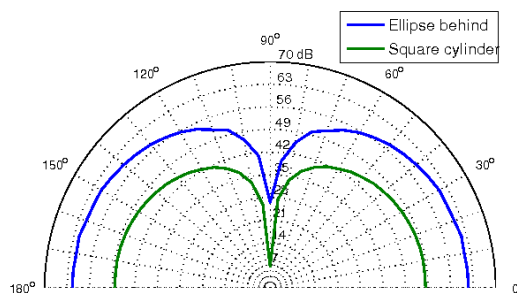


Figure 7: Directivity patterns for two cylinder profiles at radius $r = 1.0$ m on the crossflow YZ -plane

Conclusions

A FEM formulation for the hybrid computation of flow-induced noise has been presented. The numerical implementation is validated against the analytical solution of the flow-induced noise by two co-rotating vortices. A two dimensional test case computed in time and frequency domain is used to demonstrate the good performance of the PML and the robustness of the acoustic results regarding the conservative interpolation of the quantities. Additionally, three-dimensional simulations of the noise generated by wall-mounted cylinders have shown a good qualitative and quantitative agreement in comparison with experiments for the same inflow velocity.

References

- [1] C. Hahn, M. Kaltenbacher, R. Lerch, S. Becker, and F. Durst, *Influence of geometry on the generation of aeroacoustic noise*, Proceedings of ISMA, 2006, Leuven, Belgium, pp. 619–631.
- [2] M. J. Lighthill, *On sound generated aerodynamically: I. General theory*, Proc. Royal Society London **211** (1952), 564–587.